Melting transition in two dimensions: A finite-size scaling analysis of bond-orientational order in hard disks

H. Weber
Institut für Physik, Johannes-Gutenberg-Universität, Staudingerweg 7, D–55099 Mainz, Germany

D. Marx*
IBM Research Division, Zurich Research Laboratory, Säumerstrasse 4, CH–8803 Rüschlikon, Switzerland

K. Binder
Institut für Physik, Johannes-Gutenberg-Universität, Staudingerweg 7, D–55099 Mainz, Germany
(Received 23 November 1994)

We describe a general and efficient method, based on computer simulations and applicable to a general class of fluids, that allows us to determine (i) bounds on the transition densities of the melting transition that are valid in the thermodynamic limit and (ii) the order of the phase transition. The bond-orientational order parameter, its susceptibility, and the compressibility are measured simultaneously on many length scales, and the latter two quantities are extrapolated to the thermodynamic limit by application of the subblock analysis method of finite-size scaling. We include a detailed analysis, related to the subblock method, of the cross correlations of the fluctuations of the density and the order parameter. The behavior of the extrapolated order parameter susceptibility yields precise upper and lower bounds for the melting and freezing densities, respectively. We apply these techniques to the two-dimensional melting transition in large systems of 16 384 hard disks using canonical Monte Carlo computer simulations. The measured bond-orientational susceptibilities are found to be incompatible with predictions of the Halperin-Nelson-Young theory of two-dimensional melting. This and the behavior of the bond-orientational cumulant are two strong pieces of evidence of a first-order phase transition.

I. INTRODUCTION

Two-dimensional liquids have been the subject of computer simulation studies for more than 30 years. Despite their apparent simplicity, they still pose a number of challenging questions that have not been fully resolved to date. Two such issues that have attracted considerable and continued interest are the character of the melting transition[1–5] and the precise values of the transition densities for specific model fluids, see, e.g., Refs. 6 and 7. These two issues are the focus of the present paper, which deals with the simplest of these models, the hard-disk fluid.

The two-dimensional case is of particular interest because the type of order that distinguishes the solid from the liquid phase is different from that in three dimensions. In three dimensions, the solid possesses long-range positional order, i.e., the density-density correlation function decays to a finite nonzero constant at large distances. In the two-dimensional (2D) positionally ordered phase, henceforth called the 2D solid, positional order is only *quasi*-long-range, i.e., the correlation function decays algebraically to zero. This was shown by Mermin[8] in an extension of the Mermin-Wagner theorem[9] to the continuous case. As a result, no Bragg peaks in the strict sense exist in the 2D solid in the thermodynamic limit. Although it is true that Mermin's proof is strictly valid only for continuous potentials as is the case for the rigorous proof,[10] there is little reason to believe that hard disks, which have purely repulsive interaction, should possess a higher degree of order than systems whose potential has an attractive part. However, as already pointed out by Mermin, there exists a different type of order that is truly long range in the 2D solid, namely bond-orientational order. Here, "bond" denotes the imaginary line connecting the centers of two neighboring particles. A configuration possesses bond-orientational order if the angles between these bonds and an arbitrary fixed axis are correlated over arbitrary distances. Although true positional order implies bond-orientational order, the latter can exist without the former.

A melting transition in 2D was first seen in a system of hard disks in the classic computer simulation study by Alder and Wainwright.[11] From the observation of a "loop" in the density vs pressure curve, they concluded that the transition is of first order. For the freezing density, the highest possible density at which the pure fluid phase can exist, they obtained the value $\rho_f = 0.880$, and for the melting density, the lowest possible density of the solid phase, the value $\rho_s = 0.912$. (Throughout this paper we refer to densities reduced by the hard-disk diameter.) These findings were essentially confirmed by subsequent investigations by Hoover and Ree,[12] who obtained the values $\rho_f = 0.878$ and $\rho_s = 0.922$. The system sizes in these early studies did not exceed 870 particles, and the effect of the finite sizes of the sim-

ulated systems was not examined in a quantitative way. Nonetheless, the assumption of a first–order transition remained unquestioned for about a decade, until Halperin and Nelson[13,14] as well as Young[15] presented a theory of defect-mediated melting. This theory, henceforth called the HNY theory, is an extension of the ideas of Berezinskiĭ[16] and of Kosterlitz and Thouless[17] to complete melting in off-lattice models and proposes a possible alternative melting scenario. According to this theory, 2D solids might melt via two continuous phase transitions. The first transition, driven by the dissociation of dislocation pairs, transforms the solid with quasi-long-range positional order and long-range orientational order into a novel intervening phase that possesses short-range positional order and quasi-long-range orientational order. This pure phase was termed "hexatic." The unbinding of disclination pairs finally transforms the hexatic phase into an isotropic fluid in which both types of order are short range.

The HNY theory gave rise to numerous computer simulation studies of hard disks and other simple two-dimensional fluids, see Refs. 1–5 for detailed discussions and reviews. The bond-orientational order parameter was first measured in a computer simulation of a Lennard–Jones liquid by Frenkel and McTague,[18] who, however, used only 256 particles and disregarded the effects of finite system size. The size dependence of the bond-orientational order parameter was first examined by Strandburg *et al.*,[19] who measured the order parameter distribution on four different length scales. From a semiquantitative decomposition of the distributions into a solid and a fluid part, they concluded that the hard disk and the Lennard-Jones melting transitions are of first order. A more quantitative finite-size analysis of the first moment of the bond-orientational order parameter was carried out in a Lennard-Jones system of $N = 12\,480$ particles by Udink and van der Elsken[20] to determine the degree of bond-orientational order in the transition region. Again, only four different systems sizes were examined, and no measurements of the susceptibility or the cumulant were made.

Glaser and Clark,[5] recently proposed a detailed theory of the melting mechanism that yields a first-order transition. They used the *local* bond-orientational order parameter to probe the local geometry of 2D systems of strongly repulsive Weeks-Chandler-Andersen particles and of hard-core particles. Several investigations of systems of Yukawa and r^{-12} particles, which were stimulated and guided by experiments on 2D melting in colloidal systems, have been carried out by and Naidoo and co-workers[21] and by Löwen.[22] However, these two papers concentrate on issues other than the melting transition such as the impact of boundary and initial conditions and on dynamical aspects and relaxation phenomena. In none of these studies were finite-size effects taken into account on a systematic basis. Recently, careful large-scale molecular-dynamics simulations of steeply repulsive but continuous potentials, such as the r^{-12} fluid, by Andersen *et al.*[23] added new momentum to the debate. (See the outlook in the last section.)

Without having exhausted the vast literature on 2D fluids with continuous potentials,[1–5] we concentrate from now on on recent studies of the hard-disk system. In 1989, Zollweg *et al.*[6] carried out detailed investigations of large systems of hard disks (and of r^{-12} particles) using various systems sizes of up to $N = 16\,384$ particles. Their results unambiguously demonstrate a pronounced size dependence of the defect density, the shear elastic constant, the mean-square displacement, and the bond-orientational order parameter in systems of hard disks near melting. The authors draw no conclusions as to the order of the melting transition, but their work demonstrates that it may be impossible to identify the true character of the 2D melting transition without a quantitative appreciation of finite-size effects.

In view of these pronounced size effects, Zollweg and Chester[7] reexamined the early values obtained by Alder and Wainwright[11] for the transition densities. Using large systems of $N = 16\,384$ particles, they revealed that the tie line is indeed much shorter ($\rho_f = 0.887$, $\rho_s = 0.904$) than previously observed by Alder and Wainwright[11] and by Hoover and Ree.[12] However, Zollweg and Chester did not carry out a systematic quantitative finite-size analysis. Therefore, their results for the transition densities only yield an upper bound on the length of the tie line. Based on additional simulations of systems of up to 65 536 particles, they concluded that the tie line might become even shorter, or vanish entirely, if the system size is increased further.

Recently, Lee and Strandburg[24] carried out constant pressure simulations of hard disks in the vicinity of the melting transition. They measured the distribution function of the system volume, calculated the free-energy difference and carried out a Lee-Kosterlitz finite-size analysis.[25] They interpret their results as very strong evidence of a first-order transition. However, their simulated system consisted of no more than $N = 400$ particles, and the simulation possibly lacked sufficient sampling of the competing phases of different volumes; see Ref. 26 for a discussion of the "equal weight" vs the "equal height" criteria to locate the transition.

Fraser *et al.*[27] measured the edge length distribution function of Voronoi polygons in order to locate the melting transition in systems of 102 and 408 hard disks. This approach is similar in spirit to ours because it also exploits geometrical information rather than equation-of-state data. However, the analysis of Fraser *et al.* is largely qualitative. No finite-size analysis is carried out, and no numerical values are reported for the transition densities. Finally, theoretical estimates by Todo and Suzuki[28] combining the Padé approximant and the coherent anomaly method have supported previous evidence of a first-order transition in hard-core systems.

In a recent paper,[29] we used a finite-size scaling method to determine directly the order of the transition and to obtain bounds on the transition densities. Here we develop and describe this method in detail and show how it can be used in practice. At the heart of our method is the measurement of the first, second, and fourth moments of the bond-orientational order parameter distribution on a wide range of length scales obtained in simulations at only one total system size. From these moments we

calculate the susceptibility and the reduced fourth-order cumulant of the order parameter. We extract the system size dependence of the susceptibility and extrapolate to the thermodynamic limit. From the sharp increase near the transition of the susceptibility as a function of the density, we obtain upper and lower bounds of the melting and freezing densities, respectively, which are valid in the thermodynamic limit. As it turns out, the susceptibility data in conjunction with theoretical predictions also provide evidence of the order of the transition. Further independent evidence can be derived from the behavior of the order parameter cumulant as a function of density.

As our methodology is quite general in spirit, it can easily be applied to any 2D or 3D liquid, and can be combined with essentially any simulation procedure. For the sake of comparison with the largest body of detailed data available, we focused in the present study on hard disks as our model system and used standard canonical Monte Carlo simulations to obtain the ensemble averages. The hard-disk system is the minimal off-lattice model that possesses a melting transition and contains no adjustable parameters. As the potential lacks an attractive part, the system does not possess distinct liquid and gaseous phases. The disordered phase of the system is therefore termed "fluid."

The remainder of this paper is organized as follows. The main ideas of our approach are developed in the following section. In Sec. III, we discuss the technical aspects of the simulations performed. In Sec. IV A, we present the data obtained from these simulations, describe their analysis in terms of susceptibilities and compressibilities, and discuss correlations between various fluctuating quantities. Finally, Sec. IV B contains our central results concerning hard-disk melting, and a discussion of the conclusions that can be drawn from them. We summarize the paper in Sec. V and close with some speculations.

II. METHODOLOGY

A. Bond-orientational order parameter

As pointed out above, the suitable quantity for the investigation of the 2D melting transition is the global bond-orientational order parameter. It is denoted here by ψ and is defined[13,14] by

$$\psi = \left| \frac{1}{N_{\text{bond}}} \sum_i \sum_j e^{6i\phi_{ij}} \right| , \tag{1}$$

where i runs over all particles of the system, j runs over all neighbors of i, ϕ_{ij} denotes the angle between the bond connecting particles i and j and an arbitrary but fixed reference axis, and N_{bond} denotes the number of bonds in the system. The order parameter ψ is conveniently viewed as the absolute value of the sixth Fourier component of the bond angle distribution function, which is a constant in the isotropic fluid and consists of six equally spaced peaks in the solid phase. An expression for an orientational order parameter in three dimensions can be found in Ref. 30. Using this expression, our general procedures can be applied to three-dimensional fluids. The mathematically precise definition of a neighborhood in terms of a Voronoi construction is computationally very expensive. Various simpler definitions have been used in the literature.[18,30,31] It has been observed[30] that as long as the shell of next-nearest neighbors is excluded, details of the neighborhood definition have a negligible influence on the results. In the present article we define two particles to be neighbors if their distance is less than 1.3 times the hard-disk diameter.

In simple fluids, the bond-orientational order parameter ψ is expected to have the following dependence on the particle density ρ in the thermodynamic limit. It should vanish for $\rho < \rho_f$, assume a finite value less than unity at $\rho = \rho_s$, and increase towards unity as the density is increased towards the close-packing density. The behavior of ψ between the transition densities depends on the underlying melting scenario. If the transition is of first order, then, according to the lever rule, ψ should increase linearly from $\psi(\rho_f) = 0$ at ρ_f to $\psi(\rho_s)$. The HNY theory, on the other hand, predicts[13,14] that bond-orientational order should be quasi-long-range in the postulated hexatic phase, i.e., the correlation function should decay as $r^{-\eta(\rho)}$. Thus, in the thermodynamic limit, the order parameter should vanish throughout the hexatic phase. Furthermore, a jump discontinuity in ψ is predicted to occur at ρ_s.

Thus, in principle, a measurement of $\psi(\rho)$ may appear to be sufficient to determine the order of the transition. However, the measurement of the first moment of ψ alone is not sufficient for our purposes for two reasons: it provides no access to the freezing density ρ_f if the transition is of the HNY type, and, more seriously, the finite size of the simulated systems will necessarily lead to a pronounced rounding of the ψ vs ρ curve, which will render impossible the determination of either the order of the transition or the transition densities. This is demonstrated clearly by Fig. 1 in Sec. IV A. Information of greater value can be extracted from higher moments of the order parameter such as the ordering susceptibility and the corresponding fourth-order cumulant.[32] We discuss these quantities and their dependence on the system size below.

B. Ordering susceptibility

The bond-orientational susceptibility in the thermodynamic limit, denoted by χ and defined by (4) below, measures the size of the fluctuations of bond-orientational order present in the system. It should therefore show a dramatic increase as the transition densities are approached from within the pure fluid and solid phases, respectively. The precise behavior of the susceptibility at the transition points again depends on the assumed melting scenario. If the transition is of first order, the susceptibility should assume finite values (not necessarily equal) at the transition densities, and interpolate lin-

early between them. The HNY theory, on the other hand, predicts that the bond-orientational correlation function decays algebraically in the hexatic phase, and that the bond-orientational correlation length ξ

$$\xi \sim \exp\left\{b(\rho_f - \rho)^{-1/2}\right\}, \qquad \rho \to \rho_f^- \tag{2}$$

diverges as the transition density is approached from the fluid and stays infinite throughout the hexatic phase; b denotes a system-dependent constant. Because close to criticality it holds that $\chi \propto \xi^{2-\eta}$, and because η is predicted to vary between $\eta(\rho \to \rho_f^+) = 1/4$ and $\eta(\rho \to \rho_s^-) = 0$, the same behavior is expected for the susceptibility as for the correlation length. Thus, an essential singularity is predicted[13,14] for the ordering susceptibility at the freezing density ρ_f, i.e.,

$$\chi(\rho) = \hat{\chi} \exp\left\{b'(\rho_f - \rho)^{-1/2}\right\}, \qquad \rho \to \rho_f^- \tag{3}$$

as the freezing density is approached from the fluid phase; $\hat{\chi}$ and b' are system-dependent constants.

By measuring χ as a function of the density ρ, we can obtain tight upper and lower bounds on the melting and the freezing densities, respectively. A fit of (3) to our subsystem-extrapolated data for the susceptibility χ_∞ in the fluid phase, see below, will yield a HNY prediction $\tilde{\rho}_f$ of the freezing density. As we will show in Sec. IV B, this value of $\tilde{\rho}_f$, obtained under the assumption that the HNY theory correctly describes the melting of hard disks, allows us to draw conclusions as to the order of the melting transition.

We now discuss how the bond-orientational susceptibility can be measured as a function of the density. For the purpose of computer simulations, the susceptibility is most conveniently defined analogously to the common fluctuation relations

$$\chi_L = L^d \left(\langle \psi^2 \rangle_L - \langle \psi \rangle_L^2\right) \ , \tag{4}$$

where L is the linear dimension of the system under consideration and d is the dimensionality of space; as we are dealing with an athermal system, we have absorbed the usual factor of $k_B T$ into the definition of χ_L. Whereas (4) allows us to measure the susceptibility χ_L in a system of finite linear dimension L, what we require for our analysis is the susceptibility χ_∞ in the thermodynamic limit. An estimate of the latter can be obtained by measuring χ_L on a range of length scales L and extrapolating $L \to \infty$.

A series of separate simulations of systems of various total sizes would be a very computer–time intensive way to obtain data on a range of length scales. Instead, we apply the subsystem analysis method, which was originally introduced for lattice models,[32] for a review see Ref. 33, and was recently generalized to off-lattice systems.[34] Applications to the liquid-gas transition in the 2D Lennard-Jones system[34–36] as well as in a 2D fluid with internal quantum states[37,38] clearly demonstrated the power of this approach. In the present study, the subsystem method is further generalized to off-lattice simulations of solids. For each value of the density ρ, we simulate only one large system of total linear dimension S. For measurement purposes, we divide the total system into subsystems of linear dimension $L = S/M_b$, resulting in a total of M_b^2 subsystems per length scale. The length scale parameter M_b is increased in integer steps $M_b = 1, 2, \cdots$ up to a value at which the subsystem size becomes too small for a meaningful analysis. This allows us to measure, in a single simulation run, the moments of the order parameter and other averages on a wide range of length scales simultaneously. Note that periodic boundary conditions are only applied on the length scale S of the total system, i.e., properties measured in the subsystems are *not* affected by periodic boundary conditions on their length scale L.

For a given total system size S, we can now obtain an estimate of the susceptibility χ_∞ in the thermodynamic limit by observing[34,35,37,38] that, to leading order, χ_L will differ from χ_∞ by a boundary correction term of order ξ/L, i.e.,

$$\chi_L = \chi_\infty \left(1 - c\,\frac{\xi}{L}\right), \qquad L \gg \xi \ , \tag{5}$$

where c is a system-dependent dimensionless positive constant of order unity, and ξ denotes the bond-orientational correlation length. This relation is valid in the asymptotic regime where $L \gg \xi$. It can be justified as follows, see Ref. 35. The susceptibility is essentially a sum over two-bond correlation terms. Significant contributions to this sum arise only from bonds whose separation is less than the correlation length ξ. In the infinite system, *all* pairs of bonds (with a distance of less than ξ) contribute to the sum. If, however, the system is divided into subsystems, then pairs of bonds that belong to different subsystems will cease to contribute to the sum. The "forgotten" contributions will come from layers of thickness ξ about the surface of each subsystem. Provided the subsystem size L greatly exceeds the correlation length ξ, the size of these forgotten contributions will essentially be proportional to the volume ξL^{d-1} of a layer, whereas the total of the contributions will be proportional to the volume L^d of the system. Thus, the relative correction will be of order ξ/L, as stated in (5).

Given (5), an estimate of the susceptibility in the thermodynamic limit can be obtained by plotting χ_L vs L^{-1} and extrapolating from the linear region to $L \to \infty$. As a by-product of this procedure, the abscissa intercept of the extrapolation line represents an estimate of the correlation length ξ if we neglect the constant factor c, which is of order unity. The availability of the finite-size extrapolation rule (5) for the susceptibility is the main reason that the susceptibility is more useful, for the present purposes, than the order parameter itself.

Note that in the above argument we have implicitly assumed the total system to be infinitely large. As this assumption is necessarily violated in the simulation, there is a possibility that secondary finite-size effects from the size of the total system will not be captured by the extrapolation $L \to \infty$ from the subsystems.[32] Such secondary finite-size effects were observed by Hennecke[39] in simulations of a diluted Ising model. In order to check

for secondary finite-size effects and estimate their magnitude, we carried out additional simulations for one value of the density in which we varied the total system size. The results, to be presented in Sec. IV A, show that in the present case secondary finite-size effects are small in comparison with those already captured by the subsystem extrapolation.

C. Cross correlations and subsystem extrapolation

Another aspect of the subsystem analysis method that requires a more detailed discussion is that in the total system the density is constant, whereas in the subsystems the density fluctuates as a result of particles moving across subsystem boundaries. In the largest subsystems (in particular those with $M_b = 2, 3$) the density fluctuations of the various subsystems will be coupled, but in subsystems much smaller than the total system the density fluctuations can essentially be regarded as free. With the subsystem method we thus have, in a loose sense, a crossover, parametrized by M_b, from the canonical ensemble (with constant density ρ) in the total system to the grand canonical ensemble (with constant chemical potential μ) in sufficiently small subsystems. Now it is well known in statistical mechanics that, although the averages of thermodynamic observables such as the order parameter are the same in all ensembles in the thermodynamic limit, the fluctuations of the observables will in general differ from ensemble to ensemble, see, e.g., Ref. 40. In the present case, this difference may manifest itself as a difference between the susceptibilities χ_ρ and χ_μ, measured at constant density and at constant chemical potential, respectively. If such a difference exists, the crossover between the canonical and the grand canonical ensembles will be visible in the plot of χ_L vs L^{-1}. This has important consequences for the finite–size extrapolation, because care must then be taken that all data points through which we extrapolate were obtained in the same ensemble and are outside the crossover region. As only the case $M_b = 1$ is strictly canonical, and the crossover immediately starts for $M_b > 1$, it is clear that the extrapolation will have to be carried out in the grand canonical regime. This means that if χ_ρ and χ_μ differ, the first few data points with small M_b will have to be excluded from the extrapolation. Note that these complications do not arise in lattice systems because the density does not fluctuate in such systems.

Owing to the relevance of the possible difference between χ_ρ and χ_μ to the extrapolation, it is important to examine in detail the circumstances under which such a difference does in fact occur for our model. Our claim is that χ_ρ and χ_μ will differ precisely in those circumstances where the fluctuations of the density and the order parameter are correlated. Given such a correlation, the fluctuations in ψ, and hence the susceptibility, will be larger if ρ is allowed to fluctuate freely than if ρ is clamped to a constant value. This will be true regardless of whether the cross correlations $\langle \Delta\psi\, \Delta\rho \rangle$ between ψ and ρ are positive or negative. Any nonvanishing $\langle \Delta\psi\, \Delta\rho \rangle$ will lead to χ_μ being larger than χ_ρ.

In order to substantiate this claim somewhat more rigorously, we make the following phenomenological ansatz.[40] We assume that in systems whose linear dimension L is much larger than the order parameter correlation length ξ the joint probability distribution of order parameter and density can be described by the Gaussian approximation

$$P_L(\psi, \rho) \propto \exp\left\{ -\frac{L^d}{2} \left(\frac{(\Delta\psi)^2}{\chi_{L,\rho}} - \frac{\Delta\psi\, \Delta\rho}{\gamma_L} + \frac{(\Delta\rho)^2}{\kappa_{L,\psi}} \right) \right\} , \tag{6}$$

with the fluctuations $\Delta\psi = \psi - \langle\psi\rangle_L$ and $\Delta\rho = \rho - \langle\rho\rangle_L$. The susceptibility measured in a system of linear dimension L at constant density ρ is denoted by $\chi_{L,\rho}$, and γ_L is the coupling parameter measured on the same length scale L. The large-γ_L regime corresponds to weak correlations $\langle \Delta\psi\, \Delta\rho \rangle_L$. Finally, $\kappa_{L,\psi}$ denotes the compressibility measured on length scale L at a constant value ψ of the order parameter. This ansatz is correct up to interfacial free-energy contributions whenever the linear dimension L of the system is much larger than the length scale ξ of the order parameter fluctuations. In particular, it should be a good approximation in the thermodynamic limit. According to (6), ψ and ρ each fluctuate about their average values in keeping with a Gaussian distribution if the other quantity is kept constant. This is an approximation because ψ, defined in (1), is the absolute value of a multicomponent order parameter, so that the true distribution of ψ is necessarily an asymmetric Gaussian.[41] If both ψ and ρ are free to fluctuate, a coupling between them arises from the second bilinear term in the exponential, which was chosen by virtue of being the simplest form that produces such a coupling.

From (6) we can derive an expression for the difference between $\chi_{L,\rho}$ and $\chi_{L,\mu}$ by calculating the second moments of the distribution, $\langle (\Delta\psi)^2 \rangle_L$, $\langle (\Delta\rho)^2 \rangle_L$, and $\langle \Delta\psi\ \Delta\rho \rangle_L$, and solving for $\chi_{L,\mu}$ and $\chi_{L,\rho}$. The well-known result is

$$\chi_\mu - \chi_\rho = \frac{\left(L^d \langle \Delta\psi\, \Delta\rho \rangle \right)^2}{L^d \langle (\Delta\rho)^2 \rangle} , \tag{7}$$

where we have dropped the subscript L because this relation holds for finite and infinite systems alike. Furthermore, the moments in (7) are understood to be measured in the absence of constraints on ψ or ρ, i.e., at constant chemical potential μ, as realized in truly grand canonical subsystems. We therefore omit the subscript μ from the moments.

Relations such as (7) have previously been derived[42,43] by means of general thermodynamic considerations. However, we believe that the phenomenological reasoning given above makes its physical content more lucid. The relation shows that a difference between χ_ρ and χ_μ is, to lowest order, indeed a result of a correlation between ψ and ρ.

Next we identify the physical situations in which such correlations exist. As $\langle \Delta\psi\, \Delta\rho \rangle$ can be written

$$\langle \Delta\psi \, \Delta\rho \rangle = \frac{1}{\beta V} \frac{\partial \langle \psi \rangle}{\partial \mu} \ , \tag{8}$$

and the order parameter $\langle \psi \rangle$ vanishes in the fluid phase in the thermodynamic limit, no bilinear coupling should be present in the fluid phase. In the solid phase, however, the order parameter will increase monotonically with increasing density. Thus, in the solid phase a fluctuation of the density should increase the probability of an order parameter fluctuation in the same direction. As a consequence, we expect $\chi_\rho = \chi_\mu$ to hold true up to finite-size corrections not captured by the Gaussian approximation (6) in the fluid phase, but we expect $\chi_\rho < \chi_\mu$ in the solid phase. We shall return to this in Sec. IV A when we interpret our results for the susceptibility.

D. Cumulant intersection method

The second valuable quantity that involves higher moments of the order parameter distribution is the reduced fourth-order cumulant of the order parameter U_L defined as[32]

$$U_L = 1 - \frac{\langle \psi^4 \rangle_L}{3 \langle \psi^2 \rangle_L^2} \ , \tag{9}$$

where L is again the linear dimension of the subsystem under consideration, and the chosen normalization is somewhat arbitrary, see Ref. 33 for a review. The cumulant has been studied extensively for various types of phase transitions, and has frequently been used to locate transition points, see Refs. 32, 33, 38, 41, and 44–47 for applications in a variety of models. In the present study, we will use the cumulant to obtain evidence of the order of the 2D melting transition, i.e., to distinguish between the HNY critical scenario and the first-order scenario. We now discuss the behavior of the cumulant to be expected in each of these cases.

In the case of a conventional continuous phase transition, the cumulant shows the following behavior:[32,33] away from criticality, in the limit of infinite system size, the cumulant assumes different trivial limiting values in the ordered and the disordered phases. For finite systems the value of the cumulant depends on the system size: the smaller the system the more the cumulant deviates from the limiting values. At the critical point, however, the cumulant U_L assumes a nontrivial universal fixed value U^*, which in the scaling regime is independent of the system size L. As the HNY theory predicts[13–15] that the bond-orientational correlation length should diverge throughout the hexatic phase, i.e., that the hexatic phase is an extended critical phase, we would expect the cumulants for different system sizes L to collapse onto a line of fixed points $U^*(\rho)$ over the entire range of densities $\rho_f \leq \rho \leq \rho_s$ if the melting transition in the system of hard disks is of the HNY type. Concerning further details, we refer to Chap. 2. of Ref. 48 for a discussion of finite-size scaling generalized to the Kosterlitz-Thouless case, and to Chap. 10.2.3 (i) of Ref. 49 for the application of the cumulant intersection method in the framework of such transitions.

For the case of a temperature-driven first-order transition, on the other hand, a recent study[41] has shown that although the cumulants U_L for different L do not all intersect exactly at the transition point, the distance between an intersection point for finite L and the transition point in the thermodynamic limit vanishes as L^{2d} for sufficiently large system sizes. Therefore, provided the simulated systems are sufficiently large, the cumulants U_L will, within the resolution of the data, exhibit an *effective* common intersection point at the transition.

The reasoning in Ref. 41 can be carried over to the case of a density-driven first-order transition with a coexistence region. The transition density ρ_{cross} at which the cumulants U_L effectively intersect then corresponds to the density at which the phases coexist with equal statistical weight,[26] i.e., the density at which the areas under the two peaks of the bimodal order parameter distribution function are equal.

A plot of U_L vs ρ for various L, where L is sufficiently large, should thus allow us to distinguish between the proposed melting scenarios. A clear demonstration of the viability of this approach in a situation very similar to the HNY scenario has been given by Challa and Landau.[47] They performed simulations of the six-state clock model on a lattice in order to determine its phase diagram and the types of the various transitions. Between the disordered phase at high temperatures and the ordered lock-in phase at low temperatures, this model possesses an intervening XY-like critical phase of the Kosterlitz-Thouless type. It also possesses an essential singularity of the type (2) with temperature as the control parameter. In the critical phase, Challa and Landau observed, for sufficiently large systems, a clear collapse of the cumulants onto a line over an extended range of temperatures. This lattice model is probably the closest simple qualitative analogy to the HNY scenario with a fluid phase, a 2D solid phase, and the intermediate hexatic phase.

III. SIMULATIONS

We have carried out a series of canonical Monte Carlo computer simulations of systems of hard disks. It is clear that grand canonical and Gibbs ensemble simulations would be hampered in the high-densities regime, especially in the 2D solid phase. We used the standard Metropolis algorithm, which was reduced to a linear dependence of the run time on the number of particles N, with virtually no overhead, by the introduction of a "binary cell structure." These cells are chosen so small that each of them can be occupied by no more than one particle at a time. This partitioning allows efficient identification of and direct access to all potential neighbors j of a central particle i, as is required for particle moves and for the calculation of the order parameter (1).

The particle number was fixed to $N = 16\,384$ throughout the production runs. We also performed exploratory runs over 2 000 000 Monte Carlo sweeps with systems consisting of 32 400 and 65 536 particles, respectively. The area of the simulation box was kept constant during each run, and was varied from run to run to cover a range

of values of the only control parameter, the density ρ. A minimum requirement that must be satisfied during simulations of crystalline solids in order to minimize the influence of the simulation box upon the structure of the system is that the box be a unit cell of the expected crystal structure. We therefore chose a rectangular simulation box of aspect ratio $\sqrt{3}$:2. However, as Swope and Andersen[50] have argued, this condition is by no means sufficient to avoid such influence. The simulation box with its periodic boundary conditions will always constrain the net number of vacancies in the system, i.e., the number of interstitials minus the number of vacancies, to a constant value, which is not necessarily its true equilibrium value. This problem could in principle be circumvented by the application of the bicanonical simulation method proposed by Swope and Andersen;[50] unfortunately, this method requires at least an order of magnitude more computer time than conventional simulations. For the present purposes, therefore, we need to confine our investigations to the case of the net number of vacancies in the total system being equal to zero. However, we believe that this constraint has a smaller effect in the present simulation than it would have in a conventional canonical simulation. This is due to the fact that we are using the subsystem method described above. Although the canonical total system is, according to Ref. 50, not guaranteed to ever reach full equilibrium as a whole, it may still be expected to reach equilibrium locally on the length scales L of the subsystems on which the relevant measurements are carried out. The reason for this is that, unlike the periodic boundary conditions of the total system, the imaginary boundaries of the (grand canonical) subsystems impose no constraints upon the structure of the system.

The starting configurations for our simulations consisted of particles uniformly distributed over the simulation box on a triangular lattice. A rough lower bound on the time required for equilibration before the beginning of the measurements was estimated in the following way. We generated an initial configuration of an average density of $\rho = 0.892$ by placing all particles in a close-packed droplet in the middle of the simulation box, and leaving the surrounding space empty. We then measured the time required for the particles to redistribute uniformly over the box. We also examined the time evolution of the order parameter and measured the time required for the order parameter to reach a steady-state value. We obtained a lower bound of approximately 100 000 Monte Carlo sweeps (attempted 2D displacements per particle), which we chose as the *minimum* equilibration time for all densities. For each density we then equilibrated further until the block-averaged order parameter susceptibility stabilized, which took another 1 000 000 Monte Carlo sweeps for densities near the transition. Only configurations that satisfied these equilibration criteria were used for the actual measurements, extending over a minimum of another 500 000 sweeps; some runs with a considerably higher number of sweeps were carried out as additional equilibration checks. It was mainly these equilibration requirements that prevented us from choosing system sizes significantly beyond 16 384 particles.

We measured the first, second, and fourth moments of the bond-orientational order parameter defined in (1). Applying the subsystem method described above, we obtained these moments in one simulation run per value of the density over a range of length scales corresponding to values of the subsystem parameter of $M_b = 1, 2, \ldots, 32$. In order to determine a reasonable value for the frequency of measurements, we performed a preliminary run at $\rho = 0.95$ to measure the time autocorrelation function of the order parameter in the canonical total system of linear dimension S:

$$C(t) = S^2 \left[\langle \psi(0)\, \psi(t) \rangle_S - \langle \psi(0) \rangle_S^2\right] . \tag{10}$$

By fitting this data with an exponential,

$$C(t) = \hat{C}\, e^{-t/\tau} , \tag{11}$$

we obtained a rough lower bound for the autocorrelation time of $\tau \approx 50$ Monte Carlo sweeps. We then set the measurement frequency to one measurement per 20 Monte Carlo sweeps as a reasonable lower bound because measurements are relatively inexpensive compared to the particle moves. We note that the autocorrelation time is expected to increase dramatically as we move closer to the transition. The entire study required several months of CPU time on an IBM RS/6000 model 320 workstation.

IV. RESULTS AND DISCUSSION

A. Analysis of the susceptibility data

We now turn to the analysis of the measured raw data. Figure 1 shows the first moment of the order parameter ψ, measured on several length scales, as a function of the density ρ. Clearly, no accurate determination of the transition densities or of the order of the transition is possible due to pronounced finite-size rounding, especially at lower densities. Furthermore, one can clearly see that the order parameters obtained in larger subsystems show a much sharper increase as the 2D solid phase is approached. Much more insight can be gained from the behavior of the bond-orientational susceptibility χ_L, which according to (4) is calculated from the measured first and second moments of the order parameter. Figure 2 shows χ_L for various density values in the fluid phase, plotted against the inverse linear subsystem size L^{-1}. As expected, we observe an increase of χ_L with increasing subsystem size. This means that χ_L does indeed underestimate χ_∞, the extent of which increases with decreasing subsystem size, see the discussion following (5). As predicted by (5), the increase of χ_L is linear in L^{-1} for sufficiently large L. By extrapolating from the range of linear behavior to the ordinate axis, we can obtain an estimate of the susceptibility χ_∞ in the thermodynamic limit. For small values of L, we observe systematic deviations from the linear behavior. This is to be expected because the condition $L \gg \xi$ ceases to be satisfied at small values of L. The data from the total system and from the largest subsystems are subject to considerable

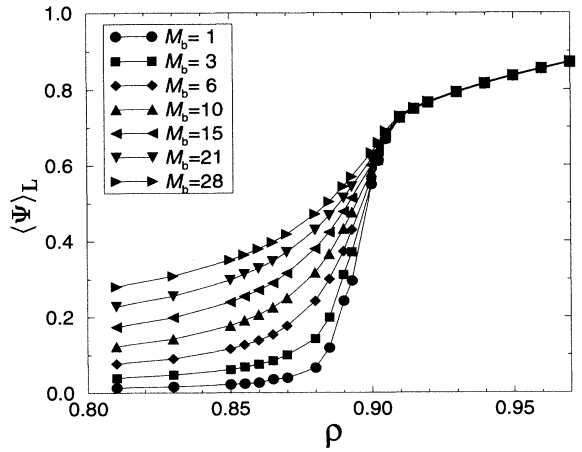

FIG. 1. First moment of the bond-orientational order parameter $\langle\psi\rangle_L$ of the hard-disk fluid as a function of density ρ for selected subbox sizes L, see inset. The subbox size parameter $M_b = S/L$ is equal to the number of subboxes along the edge of the total system. Lines are guides to the eye.

scatter because the statistics deteriorate as the subsystems become larger. Therefore, the very largest systems will be disregarded during the extrapolation procedure in the fluid range.

As the density increases and the transition region is approached from below, the minimum subsystem size that bounds the range of the linear behavior from below increases and thus the linear region becomes narrower. The closer we move to the transition, the larger the bond-orientational correlation length ξ becomes, and thus the fewer subsystem sizes fulfill the criterion $L \gg \xi$ necessary for the linear behavior of (5). The extrapolation is well controlled under this scheme because for each density it is obvious during data analysis whether the asymptotic regime has been reached with the given number of particles N. As we pointed out in Sec. II, an estimate of ξ is given (apart from an unknown positive factor c, which is of order unity) by the abscissa intercept of the extrapolation line. We find empirically that all subsystems satisfying $L \geq 2\,(c\xi)$ are well within the asymptotic regime.

We now turn to the finite-size behavior of the susceptibility in the solid phase. For small L, this behavior is similar to that observed in the fluid phase, see Fig. 3. However, there is one important difference: whereas in the fluid phase χ_L increases monotonically with L within statistical errors, it quite systematically assumes a maximum value at $M_b \approx 4$ in the solid phase. This behavior is in line with the expectation in Sec. II that $\chi_\rho \approx \chi_\mu$ in the fluid phase, whereas $\chi_\rho < \chi_\mu$ in the solid phase. We have carried out additional simulations in order to verify the picture of correlated fluctuations given in Sec. II. Figure 4 depicts a projection onto the ψ-ρ plane of the joint probability distribution $P(\psi, \rho)$ in the fluid and the solid phases, respectively. We observe that in the fluid phase the fluctuations of ψ and of ρ are uncorrelated because the position of the maximum of the distribution $P(\psi, \rho)$ with ρ fixed is independent of the value of ρ. In the solid phase, on the other hand, the fluctuations are correlated because the position of the maximum of $P(\psi, \rho)$, ρ fixed, now depends on the choice of ρ: a density fluctuation to higher densities leads, on average, to an increase of orientational order, and vice versa. Thus, Fig. 4 confirms in a qualitative manner the picture of Sec. II concerning correlated and uncorrelated fluctuations of ψ and ρ in the solid and fluid phases, respectively.

A quantitative verification can be given by checking (7) for a range of density values in the fluid and the solid phases. The value of χ_μ in the thermodynamic limit is accessible by the finite-size extrapolation from the subsystems described above. We use the value of the susceptibility measured in the total system as an estimate of χ_ρ, which is a reasonable approximation further away from the transition region. No estimate of this quantity

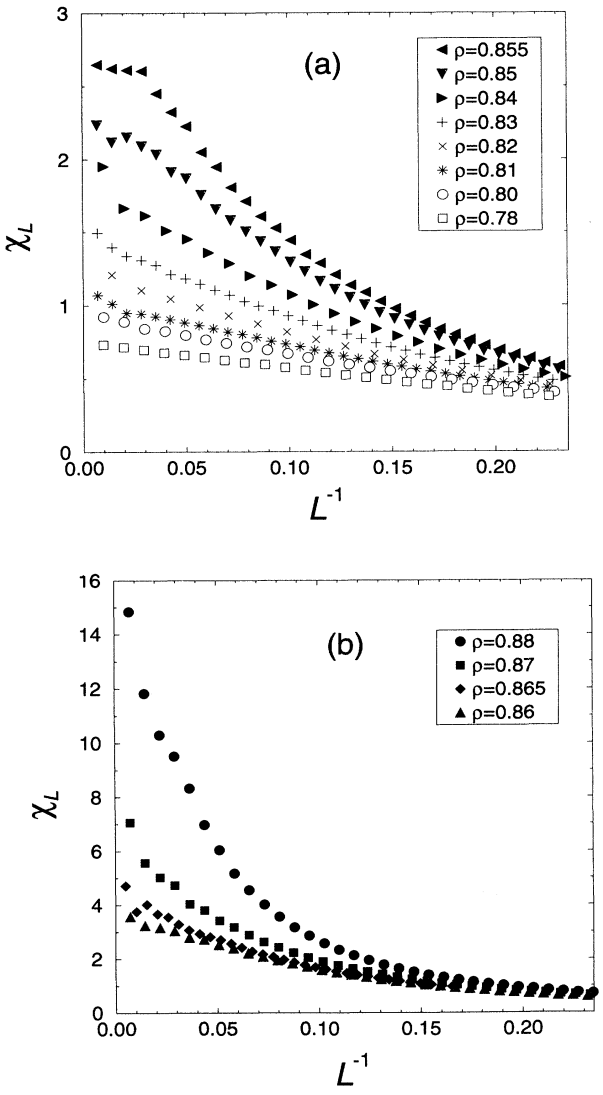

FIG. 2. Susceptibility χ_L as a function of the inverse linear subsystem size L^{-1} in the fluid phase (a) for various densities away from the transition, and (b) for densities close to the transition. Note the change of scale from (a) to (b).

in the thermodynamic limit is available here because in the spirit of the subsystem method the total system size was kept constant throughout our simulations.

By definition, the density fluctuations $L^d\langle(\Delta\rho)^2\rangle$ on the right-hand side of (7) are, up to a trivial factor of ρ^{-2}, equal to the compressibility

$$\kappa = L^d \rho^{-2} \langle(\Delta\rho)^2\rangle \ . \tag{12}$$

Again, κ is understood to be measured at constant chemical potential μ, and the subscript μ is omitted. Rovere *et al.*[34–36] have shown that the compressibility of gases and liquids away from freezing can efficiently be measured by application of the subsystem method. We have found that the method can readily be applied to dense liquids near freezing. However, the method cannot be transferred directly to the measurement of the compressibility in the solid phase. When we measure the subbox compressibility κ_L in the solid phase and plot it against the inverse linear system size L^{-1}, we observe seemingly irregular jumps, rather than the smooth, linear behavior that would allow a finite-size extrapolation. Variation of the starting configuration and of the total system size as well as extensive statistics have shown that his behavior is systematic and cannot be attributed to frozen-in disorder. The behavior can be explained by observing that within our scheme, contributions to the compress-

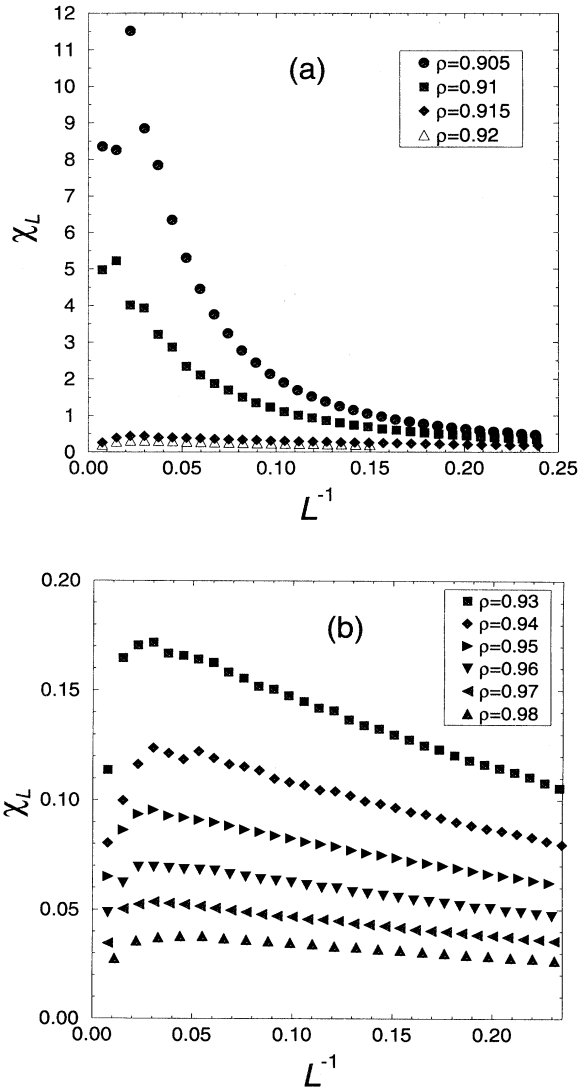

FIG. 3. Susceptibility χ_L as a function of the inverse linear subsystem size L^{-1} in the solid phase (a) for densities close to the transition, and (b) for densities away from the transition. Note the change of scale from (a) to (b).

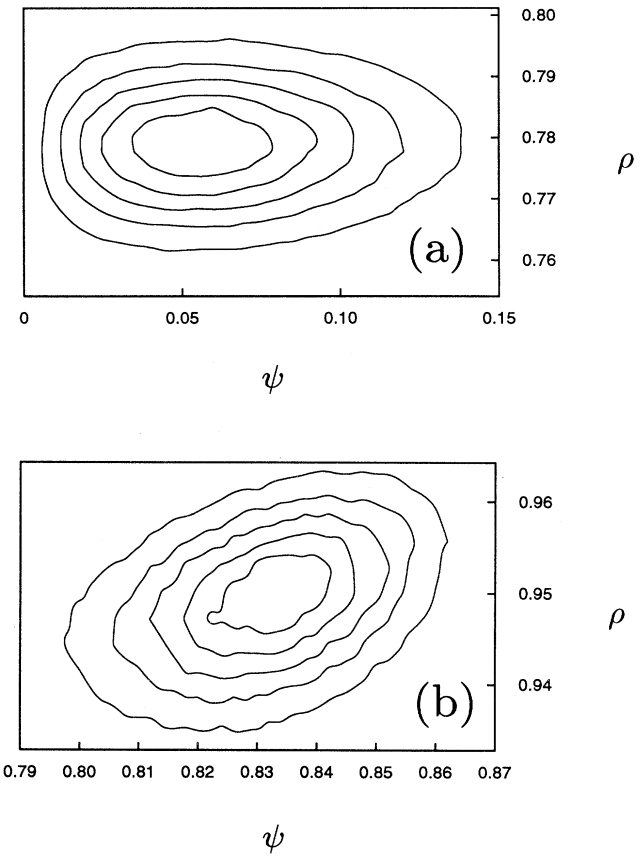

FIG. 4. Contour plot of the joint probability distribution $P(\psi,\rho)$ of the bond-orientational order parameter ψ and the *subsystem* density ρ, both measured in subsystems with M_b= 6. (a) fluid phase, density of the *total* system ρ= 0.78; from the outermost to the innermost contour, the curves correspond to $P(\psi,\rho) = 0.000\,965, 0.001\,93, 0.002\,89, 0.003\,86$, and $0.004\,82$; (b) solid phase, density of the *total* system $\rho = 0.95$; from the outermost to the innermost contour, the curves correspond to $P(\psi,\rho) = 0.000\,216, 0.000\,432, 0.000\,647, 0.000\,863$, and $0.001\,08$. Number of particles in the total system is $N = 2916$. Averages were taken over 600 000 Monte Carlo sweeps. Note that in the disordered phase the peak of $P(\psi,\rho)$ occurs at a positive value of ψ rather than at $\psi = 0$ because ψ is the absolute value of a two-component order parameter (see, e.g., Ref. 41 for a more detailed discussion of this effect). Also, the difference of resolution of abscissa scales in the ordered and the disordered phases should be taken into account when considering the size of the statistical fluctuations.

ibility in the solid arise only from fluctuations through a subbox boundary of particles located in the immediate neighborhood of such a boundary. Inspection of configurations shows that the average number of particles near a subbox wall varies significantly with the subbox parameter M_b, which leads to the observed jumps in κ_L. The jumps are thus a consequence of the incommensurability between the subbox structure and the crystal structure of the solid.

It may still be possible to obtain an estimate of the compressibility in the solid in the thermodynamic limit if we can identify some regularity in the behavior of κ_L. We have therefore modified the subsystem method by replacing the rectangular subsystems with circular ones because circular subsystems should exhibit less interference with the crystal structure. In circular subsystems the average number of particles in the immediate neighborhood of a subsystem boundary still varies systematically with the subsystem parameter, which is now the radius of the subsystem. However, the resulting variations in κ_L vs L^{-1} are now regular oscillations. They are shown in Fig. 5 for a density of $\rho = 0.95$; L is now defined by $L^2 = \pi r^2$ where r is the radius of the subsystem. Plotting $L^2\langle(\Delta\rho)^2\rangle$ vs r and comparing this to the radial distribution function $g(r)$, see Fig. 6, we find that κ_L is large wherever $g(r)$ has a point of inflection, i.e., where $g(r)$ assumes an intermediate value. The compressibility will thus be large if there is a sufficiently large number of particles near the subsystem boundary and if at the same time there is sufficient room for fluctuations. From Fig. 5 we determine κ_∞ by fitting a straight line through the maxima and one through the minima, and then extrapolating to the ordinate axis along the bisector of the angle between these two lines. The results are shown in Fig. 7 together with those obtained in the fluid phase by application of the conventional subbox method.

Finally, Fig. 8(a) shows a plot of the directly measured cross correlations $L^2\langle\Delta\psi\Delta\rho\rangle_L$ against the inverse subsystem size L^{-1} in the solid phase. In this plot the finite-size extrapolation can easily be carried out to yield

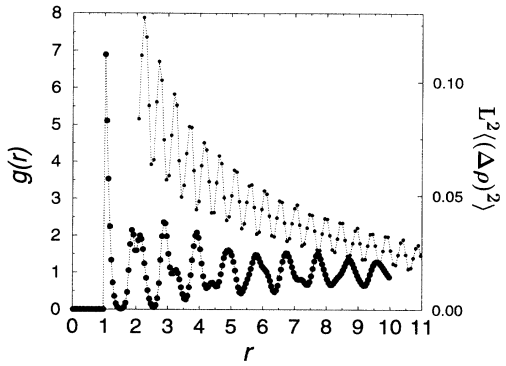

FIG. 6. Density fluctuations measured in circular subsystems as a function of the subsystem radius r (upper curve), and radial distribution function $g(r)$ measured in the total system (lower curve). Lines are guides to the eye. Minima of the density fluctuations coincide with extrema of $g(r)$. Total number of particles is $N = 576$, total density is $\rho = 0.95$.

an estimate of $L^2\langle\Delta\psi\Delta\rho\rangle_\infty$ in the thermodynamic limit. Note that because the density is a nonordering field at the melting transition, i.e., the density correlation length does not diverge, rather small sizes of the total system are sufficient to reach the asymptotic regime for the extrapolation of both $L^2\langle(\Delta\rho)^2\rangle$ and $L^2\langle\Delta\psi\,\Delta\rho\rangle$. The extrapolated values for $L^2\langle\Delta\psi\Delta\rho\rangle_\infty$ in the solid phase are plotted against the density in Fig. 8(b), whereas we find that the cross correlations essentially vanish in the fluid phase. Inserting the measured values into (7) we find that within the statistical errors of our data the equation is trivially satisfied in the fluid phase, and also satisfied in the solid phase. This demonstrates that in off-lattice systems the subsystem analysis of a single simulation run gives easy access to fluctuations and to the corresponding response quantities in various ensembles.

We have thus given a quantitative verification of the picture of coupled fluctuations. This completes the interpretation of the qualitatively different behavior of the subsystem susceptibilities χ_L as a function of L^{-1} shown

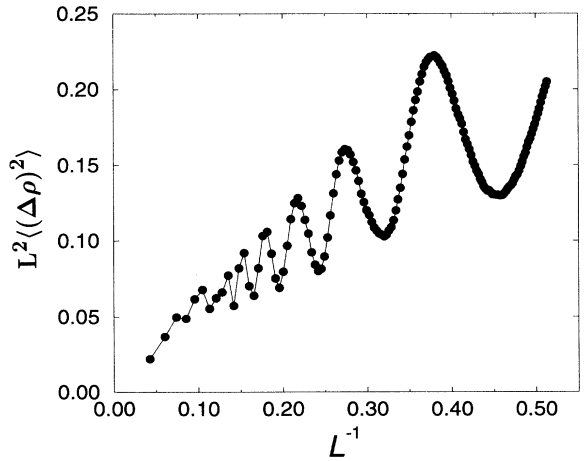

FIG. 5. Density fluctuations measured in circular subsystems of radius r as a function of L^{-1} where $L = \sqrt{\pi}r$. Total number of particles is $N = 576$, total density is $\rho = 0.95$.

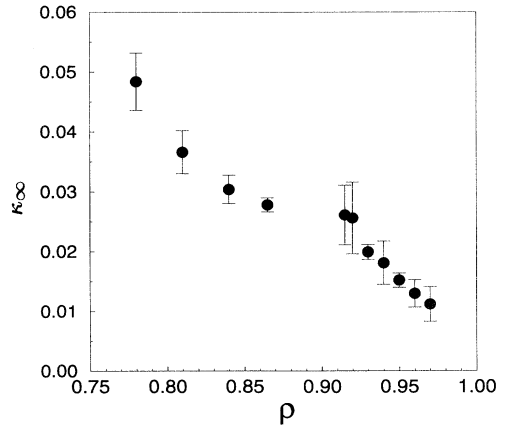

FIG. 7. Compressibility κ_∞ as a function of the density ρ, obtained by extrapolation from circular and rectangular subsystems in the solid and fluid phases, respectively. Total number of particles is $N = 576$.

in Figs. 2 and 3. We are now in a position to carry out the actual finite-size extrapolation for the susceptibility. In the fluid phase the crossover between ensembles does not manifest itself in the susceptibility, as we have shown, and does therefore not limit the range of subsystem sizes that can be included in the extrapolation. However, as pointed out above, the total system and the very largest subsystems will be excluded from the extrapolation because of their comparatively poor statistics. In addition, the influence of the boundary conditions can be assumed to be negligible in all systems apart from those with $M_b = 1, 2, 3$. For these reason, data points with $M_b \geq 4$ will be included in the extrapolation in the fluid phase.

In the solid phase, on the other hand, only those subsystems may be included that are clearly grand canonical, i.e., subsystems that are well outside the crossover region. We find empirically that this usually requires $M_b \geq 6$. For our standard total system size of $N = 16\,384$ particles, we find that the asymptotic regime is wide enough to allow a finite-size extrapolation for densities $\rho \leq 0.880$ in the fluid phase, and for $\rho \geq 0.905$ in the solid phase.

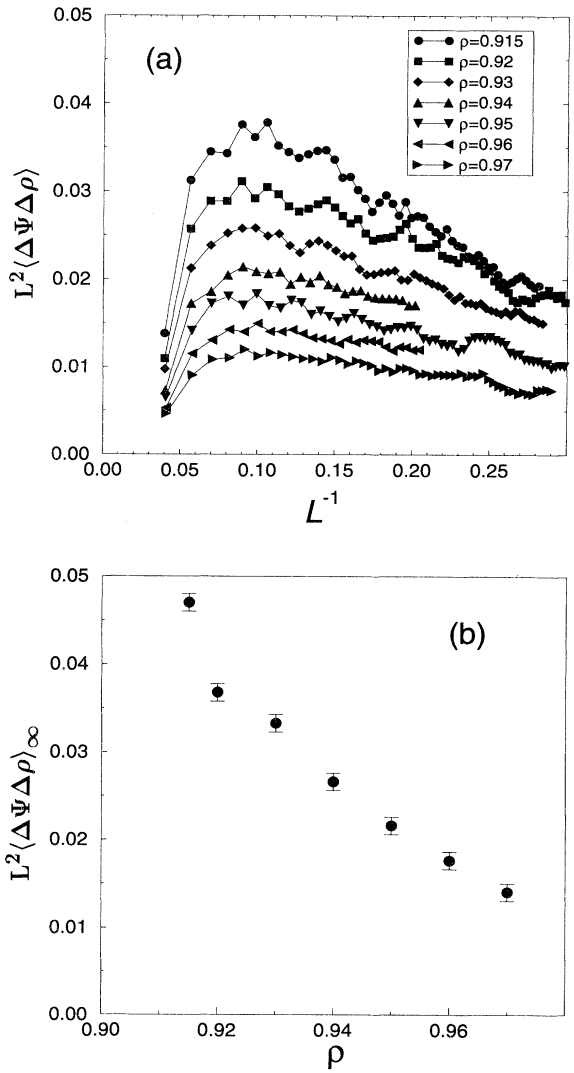

FIG. 8. Correlations between order parameter ψ and subsystem density ρ in the solid phase as a function of (a) L^{-1}, where $L = \sqrt{\pi r}$ for various total densities, and (b) the density of the total system obtained by extrapolation of the data in (a). Total number of particles is $N = 576$. Lines are guides to the eye.

In principle, another way of analyzing the susceptibility data would be a direct extraction of the critical exponent $\eta(\rho)$ using the relation

$$\chi_L \sim L^{2-\eta} \ , \tag{13}$$

which is expected to be obeyed in the hexatic phase; see Ref. 47 for such attempts in the six-state clock model. Applying this type of analysis to our data, we find that η decreases from roughly 0.4 near $\rho = 0.88$ to 0.05 at $\rho \approx 0.895$ and increases again at higher densities. However, one should not attach too much importance to the success of such double-logarithmic plots in a case where the data extend only over approximately one decade in L or less: there are examples of weak first-order transitions, e.g., the three-dimensional three-state Potts model,[41] for which such plots yield very misleading results.

We conclude this section by discussing secondary finite-size effects. Figure 9(a) shows data for the susceptibility χ_L obtained in a series of additional simulations at a solid density of $\rho = 0.95$ for which we varied the size of the total system. For each size S of the total system we have performed the subsystem extrapolation $L \to \infty$. The resulting estimates of χ_∞ are plotted against the inverse linear dimension S^{-1} in Fig. 9(b), which allows a second extrapolation $S \to \infty$ in oder to estimate the secondary finite-size effects. We observe that the L-extrapolated values for fixed S indeed possess a residual linear dependence on the inverse total system size, and that the S extrapolation leads to an increase of the susceptibility by a few percent. However, it is clear from Fig. 9(a) that the leading size corrections are satisfactorily captured by the subsystem extrapolation alone.

B. Applications to hard-disk melting

As noted above, the finite-size extrapolation procedure according to (5) yields estimates of the correlation length ξ as well as of the susceptibility χ associated with bond-orientational order. Our results for ξ and χ as functions of the density ρ are shown in Figs. 10 and 11, respectively. Both quantities show the same qualitative behavior. However, the susceptibility data, being our primary data, are of higher quality. No high-precision estimates of ξ can be obtained with the computing effort available in the present study. Note, however, that the determination of ξ from the decay of the pair correlation function is also fraught with difficulties, see Ref. 51 for examples and discussions. In addition, our procedure (5) only gives direct access to the quantity $c\xi$ and c remains unknown. Thus, in the following discussion we concentrate on our data for susceptibility. The obtained values are listed in Table I together with their estimated errors.

As expected, the susceptibility increases dramatically

as the transition region is approached from either side; qualitatively this increase is steeper on the solid side of the peak. In Fig. 11 we observe no saturation in the behavior of $\chi_\infty(\rho)$ as the densities $\rho = 0.880$ and $\rho = 0.905$ are approached from the fluid and solid sides, respectively. Thus, these values serve as conservative estimates for the maximum density at which the fluid and the minimum density at which the 2D solid phase can exist, and we arrive at the bounds

$$\rho_f > 0.880 \quad \text{and} \quad \rho_s < 0.905 \tag{14}$$

for the freezing and melting densities, respectively. These bounds are compatible with the tie line bounds obtained by Zollweg and Chester[7] in systems of $N = 16\,384$ particles, i.e., $\rho_f = 0.887$ and $\rho_s = 0.904$. Thus, our finite-size analysis supports their conclusion that the transition re-

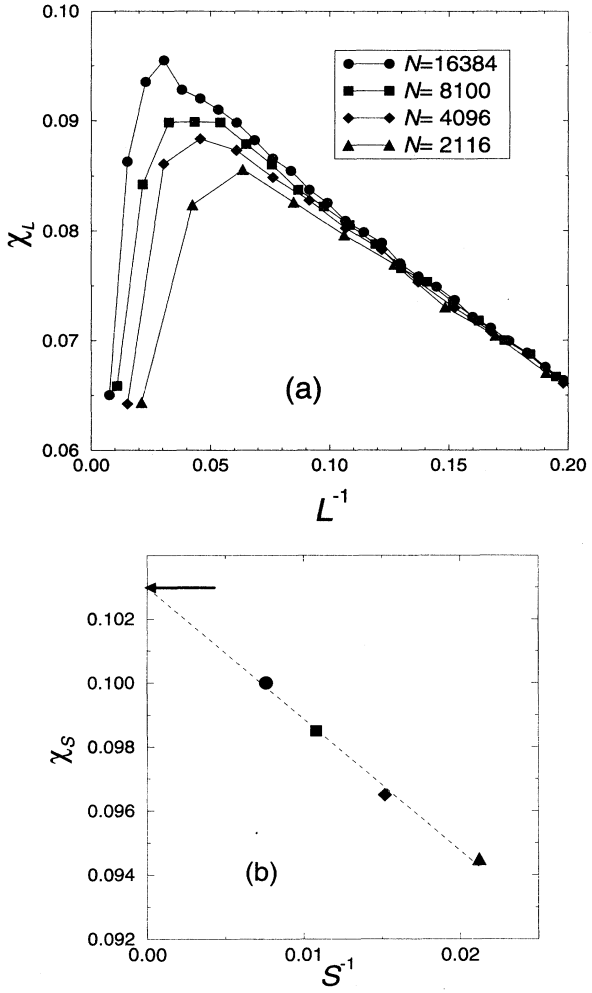

FIG. 9. Susceptibility at the total density $\rho = 0.95$ (a) as a function of the inverse linear subsystem size L^{-1} for four total numbers of particles N; lines are guides to the eye, and (b) as a function of the inverse linear total system size S^{-1} obtained from extrapolating the curves in (a); the dashed line shows the second finite-size extrapolation with respect to S, and the final value is indicated by the arrow.

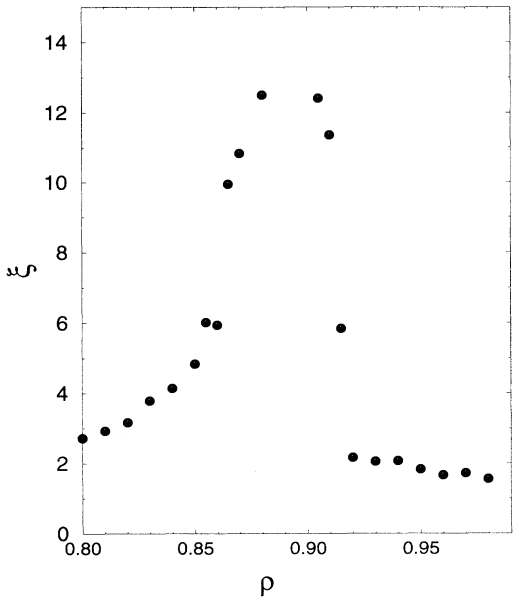

FIG. 10. Correlation length as a function of the total density ρ. The correlation length shown here is the quantity $c\xi$ obtained from relation (5). Error bars are difficult to assess and are not shown.

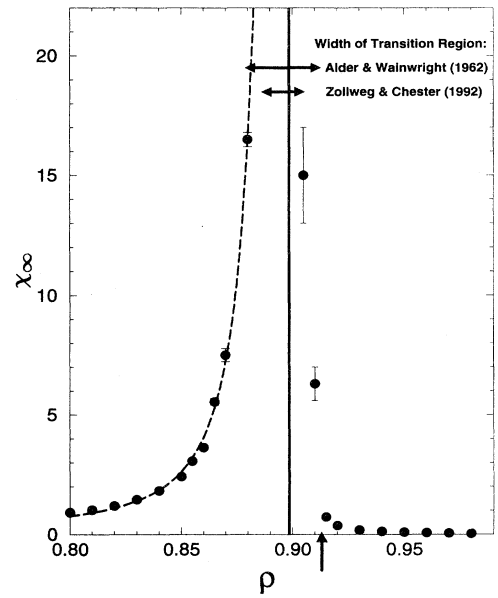

FIG. 11. Subsystem-extrapolated susceptibility χ_∞ as a function of total density ρ. The dashed line is a best fit of the HNY prediction (3) to the data in the fluid phase. The value of $\tilde{\rho}_f \approx 0.913$ obtained from the fit is indicated by a vertical arrow. The vertical solid line marks the estimate of the transition density of $\rho_{\text{cross}} \approx 0.8985 \pm 0.0005$ obtained from the cumulant intersection in Fig. 12. The widths of the arrow and of the solid line indicate the estimated errors of these quantities. The classic (Ref. 11) and best previous (Ref. 7) estimates for the tie line densities are indicated by horizontal arrows. Estimated error bars are only shown when they exceed the size of the symbols.

TABLE I. Estimates of the subsystem-extrapolated bond-orientational susceptibility χ_∞ and the estimated errors as a function of the density ρ, see Fig. 11.

ρ	χ_∞	$\Delta\chi_\infty$
0.78	0.748	0.001
0.80	0.919	0.003
0.81	1.025	0.012
0.82	1.200	0.006
0.83	1.459	0.009
0.84	1.832	0.013
0.85	2.424	0.022
0.855	3.070	0.039
0.86	3.63	0.070
0.865	5.55	0.14
0.87	7.51	0.28
0.88	16.5	0.3
0.905	15.0	2.0
0.91	6.3	0.7
0.915	0.743	0.027
0.92	0.180 0	0.009
0.93	0.134 3	0.001 1
0.94	0.134 3	0.002 1
0.95	0.099 24	0.000 30
0.96	0.074 51	0.000 16
0.97	0.056 57	0.000 19
0.98	0.041 26	0.000 11

gion is not as wide, and that the transition not as strongly first order, as was originally believed on the basis of the early results of Alder and Wainwright[11] and Hoover and Ree,[12] see Sec. I.

Further conclusions can be derived from a fit of our susceptibility data to the functional form (3) predicted by the HNY theory.[13–15] The result of the fit is shown as a dashed line in Fig. 11. Apparently, our susceptibility data can be well described by the functional form of (3). Clearly, however, the fact that our data can successfully be fitted to this highly flexible nonlinear three-parameter function does not in itself constitute evidence of continuous melting. Of much greater interest is the value of the fit parameter $\tilde{\rho}_f$, the freezing density that is obtained as a result of the fit procedure. If we include all the data points in the fluid phase in the fit, we obtain a value of $\tilde{\rho}_f = 0.913 \pm 0.001$. This value is indicated in Fig. 11 by a vertical arrow. Omitting some of the data points furthest away from the transition shifts the value resulting for $\tilde{\rho}_f$ to even higher densities (e.g., $\tilde{\rho}_f \approx 0.926$ for $0.84 \leq \rho \leq 0.88$). However, it is obvious from (14) that the densities above $\rho \geq 0.905$ belong to the solid phase. This interpretation is supported by the upper tie line bound of $\rho_s = 0.904$ reported by Zollweg and Chester[7] for 16 384 hard disks. Thus, if we assume continuous melting[13–15] to be correct, our data predict an upper density limit of the fluid phase $\tilde{\rho}_f$ that is located deeply in the solid phase, $\tilde{\rho}_f > \rho_s$. Hence, the assumption of the continuous two-step melting scenario[13–15] leads to an unphysical inconsistency in the phase diagram.

Further evidence against the HNY scenario is provided by the behavior of the fourth-order cumulant U_L. The measured values of the cumulant are plotted in Fig. 12 as a function of density for a wide range of length scales. Note that this plot shows a very narrow density range at a very high resolution of $\delta\rho/\rho \approx 0.1\%$. We observe that away from the transition the value of the cumulant is, as expected, a function of the subsystem size. The larger the subsystem, the faster the cumulant approaches the upper trivial fixed value of the perfect crystal above the transition and the lower fixed value of the isotropic fluid below the transition; note that the values of these limits depend only on the chosen normalization of U_L. At the transition, however, we observe that independently of the subsystem size L the cumulants intersect, within the resolution of our data, at a single crossing point at $\rho_{\text{cross}} = 0.8985 \pm 0.0005$. We thus observe the behavior of the cumulant that is to be expected in the case of a first-order melting transition, as outlined in Sec. II. The abscissa of the intersection point constitutes a high-precision estimate of the value ρ_{cross} of the density at which the coexisting phases have equal weight.[26] Although the observed behavior of the cumulant is, in principle, also compatible with a *single* second-order transition, this possibility will not be taken into consideration here because no such melting scenario has yet been proposed. On the other hand, our cumulant data are in blatant conflict with the prediction of the HNY melting scenario[13–15] involving two continuous transitions: we do not observe a collapse of the cumulants of all subsystem sizes onto a single line over an extended range of densities. On the basis of our data, we can rule out the existence of an extended critical phase as predicted by the HNY theory down to the scale of 0.001 hard-disk density units.

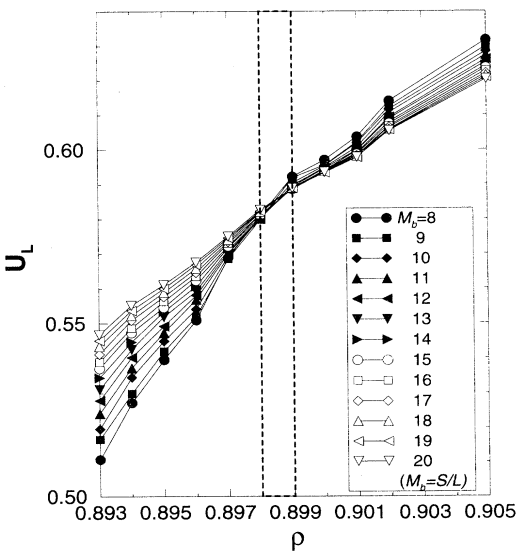

FIG. 12. Order parameter cumulants U_L as a function of the total density ρ for various subsystem sizes $L = S/M_b$. The lines connecting the data points are guides to the eye. The vertical dashed lines mark the range within which the cumulant intersection occurs, i.e., they indicate the error in the estimated transition density of $\rho_{\text{cross}} \approx 0.8985 \pm 0.0005$.

V. SUMMARY AND OUTLOOK

In this paper we have devised a package of techniques that allows the determination of (i) precise bounds for the liquid to solid phase boundaries containing corrections for the finite size of the simulated system, and (ii) the order of the phase transition. The method yields estimates of the compressibility, of the bond-orientational susceptibilities (in both the canonical and the grand canonical ensembles), and of the correlation length from a single type of simulation. Our method can be applied to a broad class of model fluids in two and three dimensions, and can be combined with various computer simulation techniques.

We have studied in detail the features of the subsystem analysis method applied to off-lattice systems and have devised a way to finite-size extrapolate from the subsystem averages. We have shown that this efficient method can be applied to dense fluids, as well as to solid systems in the vicinity of the melting transition. In particular we have demonstrated how to obtain estimates of the compressibility in the solid phase extrapolated to the thermodynamic limit. This allowed us to show that the fluctuations of density and bond-orientational order parameter are correlated in the 2D solid phase, but essentially uncoupled in the fluid phase.

Specifically, we have used the above finite-size scaling techniques in order to investigate the melting transition of hard disks. We have obtained thermal averages of the bond-orientational order parameter, its susceptibility, and its fourth-order cumulant in large systems of hard disks over a wide range of length scales in a narrow density window near melting. We have then extrapolated the susceptibilities obtained in the subsystems to the thermodynamic limit. An important virtue of our method is that it is clearly visible during data analysis for each set of parameters to what extent the measured data warrant any statements about the behavior in the thermodynamic limit. In the present series of simulations, it has been possible to obtain high-quality finite-size-scaled data for densities as high as $\rho = 0.880$ in the fluid phase, and as low as $\rho = 0.905$ in the solid phase. These are also our lower and upper bounds for the freezing and melting densities, respectively. Investing additional computing time it would be no problem in principle to obtain even tighter bounds. With respect to the order of the melting transition we find the following: a fit of our susceptibility data to the relevant prediction of the Halperin-Nelson-Young theory of two-step continuous melting leads to an unphysical inconsistency, and our cumulant data show that, down to a resolution in density of 0.001 hard-disk units, no extended critical phase exists between the fluid and the solid phases. Thus, under the assumptions that the equilibrium net number of vacancies is approximately equal to zero, and that size of the simulated systems of $N = 16\,384$ particles is sufficient to capture the relevant physical effects, our finite-size analysis yields two independent pieces of evidence that the melting transition of hard disks is of first order. Together with previous pieces of evidence from large-scale computer simulations[5,7,24] it now seems, more than thirty years after the discovery of the hard-disk transition by Alder and Wainwright,[11] to be well established that the 2D hard-disk solid melts via a conventional first-order transition.

This conclusion is particularly remarkable in view of recent findings by Andersen *et al.*,[23] who are currently undertaking large-scale molecular dynamics simulations of 2D soft repulsive isotropic particles that interact, e.g., via a r^{-12} potential. In this system they have observed equilibrium states that possess the structural properties of the hexatic phase postulated by the HNY theory. This difference to the hard-disk fluid is interesting in view of a trend established for the 3D soft-disk case by Hoover *et al.*,[52] see also Ref. 53. They performed a comparative study of various r^{-n} potential systems in 3D with $n = 4, 6, 9, 12, \infty$, and found that the fractional density change and free-energy difference upon melting increase significantly with increasing "hardness parameter" n. Thus, in 3D, the softer the purely repulsive potential, the less strongly first order the melting transition. Moreover, note that the HNY theory involves a number of parameters such as elastic constants that are system dependent. The theory predicts that the proposed two-stage melting scenario will materialize only in those systems in which these constants lie within certain ranges. Other systems may melt according to different scenarios. In particular, they may undergo a first-order transition, see also the very instructive Figs. 20 and 21 of Nelson's review article.[1] To our knowledge, it has not been possible to date to calculate these constants analytically for a single model fluid, and thus to determine within the HNY theory the type(s) of transition the systems of interest should undergo. However, based on the results of the present study in conjunction with the findings of Andersen *et al.*, one is tempted to speculate that there might indeed exist a *qualitative* difference between the melting scenarios of the hard–disk limit and of some continuous potentials. A *lattice* model of defect melting that exhibits such a crossover from a single first-order transition to two-step melting as a function of a certain parameter has been devised and investigated by Janke and Kleinert, see Ref. 54 and references therein. The translation of such ideas to the concepts that are commonly used to describe off-lattice fluids, such as type and range of the interaction potential, would certainly be a challenge for future research.

Finally, we feel that the limitations of the present study, i.e., the maximum total system size of $N = 16\,384$, the equal numbers of vacancies and interstitials, the systematic errors caused by the secondary size effects, and the fact that the range of subsystem sizes L was somewhat too small to allow for high-precision extrapolations to $L \to \infty$, are no limitations of principle of the method proposed in this paper, but can be alleviated as one gains greater access to significantly more powerful computers, such as high-speed parallel supercomputers. A large-scale computational investigation of two-dimensional melting for continuous potentials on such an advanced machine along the lines of the present study should be illuminating.

Note added in proof. Recently, Ryzhov and Tareyeva[55] have carried out density functional calculations to obtain first-principles estimates for the stability limits of the

hard-disk solid and hexatic. Their results rule out the existence of a hand-disk hexatic.

ACKNOWLEDGMENTS

We thank David Nelson, Hans Andersen, and Wolfhard Janke for stimulating discussions and remarks, as well as Hans Andersen for sharing results with us prior to publication. D.M. gratefully acknowledges his Forschungsstipendium by the Deutsche Forschungsgemeinschaft and his postdoctoral research grant from IBM.

* Present address: Max-Planck-Institut für Festkörperforschung, Heisenbergstrasse. 1, D–70569 Stuttgart, Germany.

[1] D. R. Nelson, in *Phase Transitions and Critical Phenomena*, edited by C. Domb and J. L. Lebowitz (Academic, London, 1983), Vol. 7.
[2] K. J. Strandburg, Rev. Mod. Phys. **60**, 161 (1988).
[3] H. Kleinert, *Gauge Fields in Condensed Matter* (World Scientific, Singapore, 1989), Vol. II, Part III, Chap. 14.
[4] *Bond-Orientational Order in Condensed Matter Systems*, edited by K. J. Strandburg (Springer, Berlin, 1992).
[5] M. A. Glaser and N. A. Clark, Adv. Chem. Phys. **83**, 543 (1993).
[6] J. A. Zollweg, G. V. Chester, and P. W. Leung, Phys. Rev. B **39**, 9518 (1989).
[7] J. A. Zollweg and G. V. Chester, Phys. Rev. B **46**, 11 187 (1992).
[8] N. D. Mermin, Phys. Rev. **176**, 250 (1968).
[9] N. D. Mermin and H. Wagner, Phys. Rev. Lett. **17**, 1133 (1966).
[10] J. Fröhlich and C. Pfister, Commun. Math. Phys. **81**, 277 (1981).
[11] B. J. Alder and T. E. Wainwright, Phys. Rev. **127**, 359 (1962).
[12] W. G. Hoover and F. H. Ree, J. Chem. Phys. **49**, 3609 (1968).
[13] B. I. Halperin and D. R. Nelson, Phys. Rev. Lett. **41**, 121 (1978).
[14] D. R. Nelson and B. I. Halperin, Phys. Rev. B **19**, 2457 (1979).
[15] A. P. Young, Phys. Rev. B **19**, 1855 (1979).
[16] V. L. Berezinskiĭ, Zh. Eksp. Teor. Fiz. **59**, 907 1990 [Sov. Phys. JETP **32**, 493 (1971)]; **61**, 1144 (1971) [**34**, 610 (1972)].
[17] J. M. Kosterlitz and D. J. Thouless, J. Phys. C **5**, L124 (1972); **6**, 1181 (1973).
[18] D. Frenkel and J. P. McTague, Phys. Rev. Lett. **42**, 1632 (1979).
[19] K. J. Strandburg, J. A. Zollweg, and G. V. Chester, Phys. Rev. B **30**, 2755 (1984).
[20] C. Udink and J. van der Elsken, Phys. Rev. B **35**, 279 (1987).
[21] K. J. Naidoo, J. Schnitker, and J. D. Weeks, Mol. Phys. **80**, 1 (1993); K. J. Naidoo and J. Schnitker, J. Chem. Phys. **100**, 3115 (1994); see also J. J. Morales, E. Velasco, and S. Toxvaerd, Phys. Rev. E **50**, 2844 (1994).
[22] H. Löwen, J. Phys. Condens. Matter **4**, 10 105 (1992).
[23] H. C. Andersen, K. Bagchi, and W. C. Swope (private communication).
[24] J. Lee and K. J. Strandburg, Phys. Rev. B **46**, 11 190 (1992).
[25] J. Lee and J. M. Kosterlitz, Phys. Rev. Lett. **65**, 137 (1990).
[26] C. Borgs and R. Kotecký, J. Stat. Phys. **61**, 79 (1990); Phys. Rev. Lett. **68**, 1734 (1992); C. Borgs and W. Janke, *ibid.* **68**, 1738 (1992); W. Janke, Phys. Rev. B **47**, 14 757 (1993); C. Borgs and S. Kappler, Phys. Lett. A **171**, 37 (1992).
[27] D. P. Fraser, M. J. Zuckermann, and O. G. Mouritsen, Phys. Rev. A **42**, 3186 (1990).
[28] S. Todo and M. Suzuki, J. Phys. Soc. Jpn. **63**, 3552 (1994).
[29] H. Weber and D. Marx, Europhys. Lett. **27**, 593 (1994).
[30] P. J. Steinhardt, D. R. Nelson, and M. Ronchetti, Phys. Rev. B **28**, 784 (1983).
[31] J. S. van Duijnefeldt and D. Frenkel, J. Chem. Phys. **96**, 4655 (1992).
[32] K. Binder, Z. Phys. B **43**, 119 (1981).
[33] K. Binder, Ferroelectrics **73**, 43 (1987).
[34] M. Rovere, D. W. Heermann, and K. Binder, Europhys. Lett. **6**, 585 (1988).
[35] M. Rovere, D. W. Heermann, and K. Binder, J. Phys. Condens. Matter **2**, 7009 (1990).
[36] M. Rovere, P. Nielaba, and K. Binder, Z. Phys. B **90**, 215 (1993).
[37] D. Marx, P. Nielaba, and K. Binder, Phys. Rev. Lett. **67**, 3124 (1991).
[38] D. Marx, P. Nielaba, and K. Binder, Phys. Rev. B **47**, 7788 (1993).
[39] M. Hennecke, Phys. Rev. B **48**, 6271 (1993).
[40] L. D. Landau and E. M. Lifshitz, *Statistical Physics*, 3rd ed. (Pergamon Press, Oxford, 1980), Pt. 1.
[41] K. Vollmayr, J. D. Reger, M. Scheucher, and K. Binder, Z. Phys. B **91**, 113 (1993).
[42] J. L. Lebowitz, J. K. Percus, and L. Verlet, Phys. Rev. **153**, 250 (1967).
[43] M. P. Allen and D. J. Tildesley, *Computer Simulations of Liquids* (Oxford Science Publications, Clarendon Press, Oxford, 1987).
[44] K. Binder and D. P. Landau, Phys. Rev. B **30**, 1477 (1984).
[45] M. S. S. Challa, D. P. Landau, and K. Binder, Phys. Rev. B **34**, 1841 (1986).
[46] D. Marx, S. Sengupta, O. Opitz, P. Nielaba, and K. Binder, Mol. Phys. **83**, 31 (1994).
[47] M. S. S. Challa and D. P. Landau, Phys. Rev. B **33**, 437 (1986).
[48] M. N. Barber, in *Phase Transitions and Critical Phenomena* (Ref. 1), Vol. 8.
[49] K. Binder in *Monte Carlo Methods in Statistical Physics*, 2nd ed., edited by K. Binder (Springer, Berlin, 1986).
[50] W. C. Swope and H. C. Andersen, Phys. Rev. A **46**, 4539 (1992); J. Chem. Phys. **102**, 2851 (1995).
[51] O. Opitz, D. Marx, S. Sengupta, P. Nielaba, and K. Binder, Surf. Sci. Lett. **297**, L122 (1993); W. Janke and S. Kappler,

Nucl. Phys. B **34**, 674 (1994).
[52] W. Hoover, S. G. Gray, and K. W. Johnson, J. Chem. Phys. **55**, 1128 (1971).
[53] J. D. Weeks and J. Q. Broughton, J. Chem. Phys. **78**, 4197 (1983).
[54] W. Janke and H. Kleinert, Phys. Rev. Lett. **61**, 2344 (1988); **62**, 608(E) (1989); Phys. Rev. B **41**, 6848 (1990).
[55] V. N. Ryzhov and E. E. Tareyeva, Phys. Rev. B **51**, 8789 (1995).